Properties of Sodium Carbonates Beds at Incipient Fluidization and Terminal Velocities of Solids

M. HARTMAN*, O. TRNKA, V. VESELÝ, and K. SVOBODA

Institute of Chemical Process Fundamentals, Academy of Sciences of the Czech Republic, CZ-165 02 Prague

Received 26 July 2000

An 8.5 cm i.d. column was employed to measure in air the minimum fluidization velocity and the terminal velocity of different sodium carbonates particles of mean size ranging from 0.14 mm to 0.72 mm. Based upon the amassed experimental data, correlations were developed to estimate these fundamental fluidization characteristics which delineate modes of gas-solid contacting.

The need to reduce the emission of different acidic pollutants to the atmosphere has led to extensive research on their removal from waste and flue gases. While large-scale cleaning processes usually employ relatively inexpensive calcium- or magnesium-based sorbents, potential of Na_2CO_3 should also be explored. Such very effective materials can be employed for capture of gaseous, weak acidic pollutants and difficult odours. Experimental results of *Svoboda et al.* [1] and *Mocek et al.* [2] on low-temperature sorption of nitrogen oxides by Na_2CO_3-based sorbents are quite promising.

A practical way of contacting gases (or liquids) with particulate solids is provided by a fluidized bed. Because of intensive solids mixing, temperature fields are nearly uniform within the whole volume of bed. Hot or cold spots do not occur in the bed and the heat transfer as well as the mass transfer are usually rapid.

The mode of fluidization or the regime of fluidized beds varies widely from the state of minimum fluidization to pneumotransport in dependence on the size, density, and shape of particles, on the flow rate and physicochemical properties of an employed fluid. The regimes are so different that they cannot be represented by a single hydrodynamic model [3].

From an engineering point of view, two basic hydrodynamic states of a given bed should always be considered: the onset of fluidization which occurs at the minimum fluidization velocity [4] and beginning entrainment that is more or less close to the terminal (free fall) velocity of the smallest particles in the bed [5]. Moreover, knowledge of the minimum fluidization makes it possible to model the performance of a fluidized-bed (bubbling) reactor since it permits the prediction of the amount of gas which passes through the bed in the form of bubbles.

While some data on the fluidized beds of limestone-based materials can be found in the literature [6, 7] there is little known about fluidized beds with sodium carbonate particles. In the present study, the investigation has been undertaken to explore the particle density and porosity, the minimum fluidization and entrainment velocities for sodium carbonate decahydrate (SCD, $Na_2CO_3 \cdot 10H_2O$), for its calcination (dehydration) products sodium carbonate monohydrate (SCM, $Na_2CO_3 \cdot H_2O$) and anhydrous sodium carbonate (ASC, Na_2CO_3).

EXPERIMENTAL

The present study was conducted with an anal. grade sodium carbonate decahydrate (SCD) produced by Fluka (Switzerland) and its calcines (monohydrate (SCM) and anhydrous carbonate (ASC)). The particles of SCM and ASC were prepared by dehydrating particulate SCD at 30 °C and 70 °C, respectively, for 2 h in a muffle furnace in a slow stream of dried air. On dehydrating, the particles were sieved carefully and maintained in airtight containers.

The true (skeletal) and apparent densities of these materials were determined by the helium and mercury pycnometry (AutoPore, Micromeritics, USA). The physicochemical properties of the three explored solids are presented in Table 1. The particles comprised six very narrow, carefully sieved fractions: 0.125—0.16 mm ($\bar{d}_p$ = 0.142 mm), 0.20—0.25 mm ($\bar{d}_p$ = 0.225 mm), 0.315—0.40 mm ($\bar{d}_p$ = 0.357 mm), 0.40—0.50 mm ($\bar{d}_p$ = 0.45 mm), 0.50—0.63 mm ($\bar{d}_p$ = 0.565 mm), and 0.63—0.80 mm ($\bar{d}_p$ = 0.715 mm). The Czech Standard series of sieves was employed, in which the apertures of the adjacent sieves are arranged in multiples of approximately 1.25.

The screen size or sieve size, $\bar{d}_p$, used in this work

*The author to whom the correspondence should be addressed.

Table 1. Properties of Particulate Sodium Carbonates

Property	SCD	SCM	ASC
Mass loss on calcination[a]	–	0.5666	0.6296
True (skeletal) density, $\rho_t/(\text{kg m}^{-3})$	1390.	2200.	2500.
Apparent density, $\rho_s/(\text{kg m}^{-3})$	1390.	611.5	527.5
Porosity, e	0	0.7220	0.7890
Pore volume, $V_p/(\text{m}^3\ \text{kg}^{-1})$	0	1.181×10^{-3}	1.496×10^{-3}

a) Related to $Na_2CO_3 \cdot 10H_2O$ as a parent material.

is the arithmetic mean of the aperture of the screen which just lets the particles pass through and the next finer screen below on which they are retained.

Examination with an optical microscope indicated that the collected particles had approximately equal axes at right angles to each other. In other words, their near-isometric form can be assumed. While sharp edges could be seen on the SCD material, the calcined or dehydrated SCM and ASC particles appeared more or less round.

To take into account the particle shape, the sphericity was employed as the most appropriate single measure for characterizing the shape of close-to-isometric nonspherical particles. For the definition and features of the sphericity, a reader is referred to the literature [4, 5, 8]. For example, the sphericity, $\psi = 1$ for perfect spheres, and $0 < \psi < 1$ for other bodies.

Particle sphericity was determined by a procedure based upon measurements of pressure drop across the fixed (static) bed [9]. According to this method, the particle sphericity can be expressed from the widely accepted Ergun equation [4, 10]

$$(\Delta P/\Delta H)\psi^2 - [1.75(1-\varepsilon)\rho_f U^2/(\varepsilon^3 d_p)]\psi - \\ -150(1-\varepsilon)^2\mu_f U/(\varepsilon^3 d_p^2) = 0 \qquad (1)$$

The bed voidage, ε, was determined experimentally by weighing a mass of particles slowly poured into a glass cylinder.

$$\varepsilon = 1 - W/[FH(\rho_s - \rho_f)] \qquad (2)$$

The average values of poured bed voidage for SCD, SCM, and ASC amounted to 0.55, 0.48 and 0.45, respectively.

The values of the particle sphericity, ψ, fluctuated slightly for different particle size. Repeated measurements provided average values of the sphericity, $\psi = 0.63$ for SCD, $\psi = 0.82$ for SCM, and $\psi = 0.85$ for ASC. Dried air was used at 20°C as an operation medium (density, $\rho_f = 1.20$ kg m^{-3}; viscosity, $\mu_f = 1.81 \times 10^{-5}$ Pa s).

An experimental set-up with a glass column of inside diameter 8.5 cm and height 2 m was used. The column was equipped with an interchangeable gas plate distributor and fluidizing grid. Their free area was varied to avoid excessive pressure drop. The distance between these perforated plates was 3 cm. A ring with a height of 1.5 cm was situated just above the fluidizing grid for measurements of the pressure drop across the bed. The elutriated particles were separated in a cyclone, and the dust was removed in a fabric filter. The flow rate of air was gradually increased (or decreased), and the pressure drop of the fluidized bed *vs.* the velocity of air was recorded.

The points of minimum (incipient) fluidization and the terminal velocities of very narrow fractions of SCD, SCM, and ASC particles determined from the dependence of pressure drop across the bed *vs.* gas (air) velocity for a shallow bed of such particles were determined by experiment in a glass fluidization column [8, 11, 12].

All tested powders behaved according to the "normal" curve and began "to bubble" as soon as the minimum fluidization velocity, U_{mf}, had been exceeded. The terminal velocities given in this work are the arithmetic mean of the velocity at which the decline in pressure drop becomes noticeable and that when practically all the particles are entrained out of the column. Such values are related to the mean sieve size of the particles.

The difference between the end and the beginning of entrainment is a function of the width of a sieved fraction (0.035—0.17 mm) and varies from about 0.05 m s^{-1} for the smallest particles to approximately 0.25 m s^{-1} for the largest ones. Replicate measurements of minimum fluidization velocity and the terminal velocity showed reproducibility better than 4 %.

RESULTS AND DISCUSSION

The measured minimum fluidization velocities of the SCD, SCM, and ASC particles vary from 0.004 m s^{-1} to 0.190 m s^{-1} for particles in the range of 0.14—0.72 mm. These results are plotted in Fig. 1 as a function of the mean particle size, $\bar{d}_p$. As can be seen, the presented dependences are not linear. The SCD beds commence fluidizing at the highest superficial gas velocities because of their highest density. In Fig. 2, the experimental data points are replotted in terms of the dimensionless variables such as the Archimedes number, Ar, and the Reynolds number, Re_{mf}. We can see in this figure that the results for the three tested materials follow approximately a single dependence.

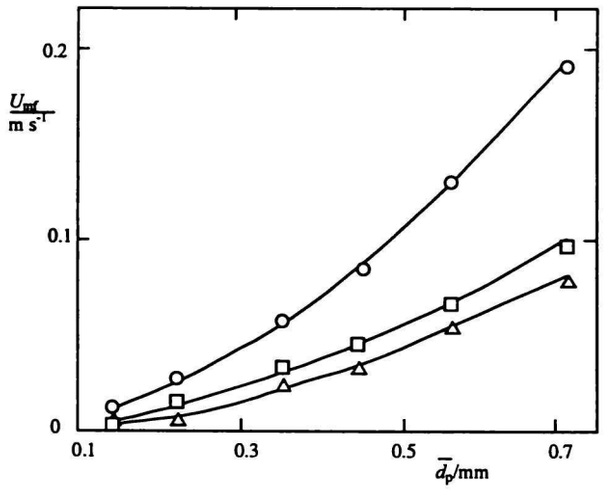

Fig. 1. Measured and predicted minimum fluidization velocities: ○ SCD; □ SCM; △ ASC; the lines show predictions of eqn (*4*) for the respective materials.

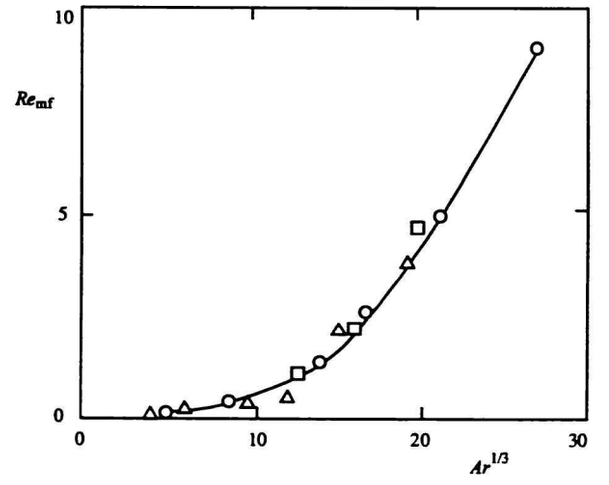

Fig. 2. Measured and predicted points of minimum fluidization. The symbols are the same as in Fig. 1.

In an effort to represent our experimental findings, we fitted an empirical quadratic expression, based on the Ergun model [4, 10]

$$k_2 Re_{mf}^2 + k_1 Re_{mf} - Ar = 0 \qquad (3)$$

to our measured data on the point of minimum fluidization. The numerical constants were determined from the whole set of the collected data by the simplex optimization method

$$56.35 Re_{mf}^2 + 1616 Re_{mf} - Ar = 0 \qquad (4)$$

The U_{mf} and Re_{mf} values computed from eqn (*4*) agree well with the directly measured values within an average deviation and a maximum deviation of ±2.8 % and ±4.7 %, respectively. The computed lines are also shown in Figs. 1 and 2. Consequently, the correlation (*4*) is proposed here as a means of interpolation of U_{mf} within the range of the operating variables involved in this work. We believe that such interpolated and cautiously extrapolated values are reliable enough for engineering design calculations.

In contrast to the Ergun relation (*1*) derived by consideration of pressure drop [4, 10], *Wen* and *Yu* [13] developed a correlation on the basis of drag force considerations. Their correlation, after modification to apply to nonspherical particles, takes the form

$$2.70\psi^{0.687} Re_{mf}^{1.687} + 18 Re_{mf} - \psi^2 \varepsilon_{mf}^{4.7} Ar = 0 \qquad (5)$$

Computed values of U_{mf} from eqn (*5*) agree with the experimental values with an average deviation of ±27 %, while the deviations vary from ±15 to ±32 %.

While information on the incipient state of fluidization is quite satisfactory, with a number of equations and amount of experimental data to be found in the literature, this is not so for the terminal velocity. The reason for this state of the art is the obvious difficulty of measuring the terminal velocity and of describing real gas-solid particle systems theoretically.

Although we have worked with the very carefully sieved fractions as narrow as possible, they are not rigorously of uniform size and shape. The terminal velocity was related to the mean mesh size of particles. It represents, therefore, the parameter of the bed material rather than the true, free-fall velocity of a single particle in an indefinite medium.

The measured terminal velocities varied from about 0.25 m s^{-1} to approximately 3 m s^{-1} and are shown in Fig. 3. As can be seen in Fig. 4, the experimental data points form practically a single curve

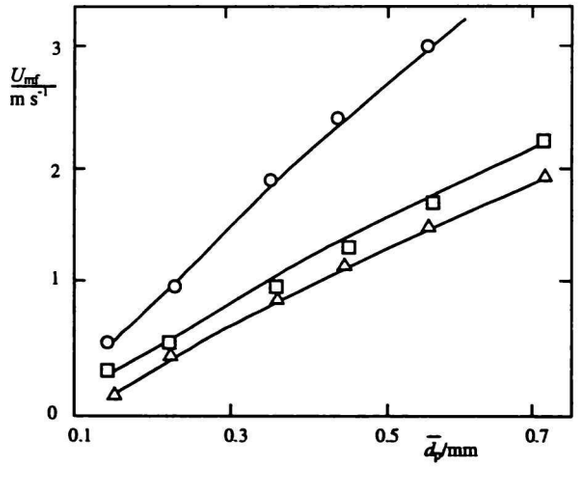

Fig. 3. Measured and predicted values of terminal velocities. The symbols are the same as in Fig. 1, the lines show predictions of eqn (*6*).

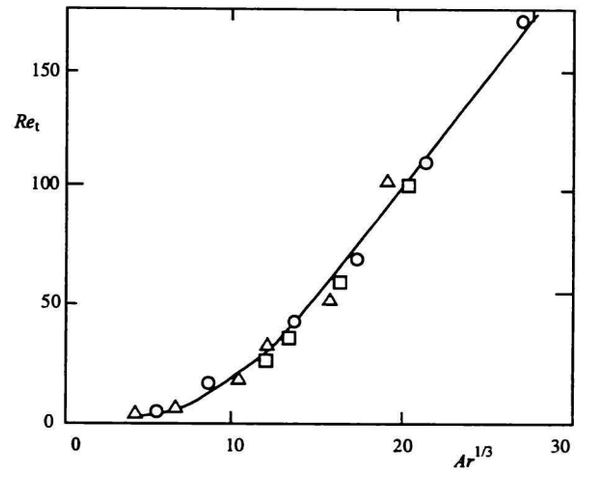

Fig. 4. Measured and predicted values of the Reynolds number at terminal velocity. The symbols are the same as in Fig. 1.

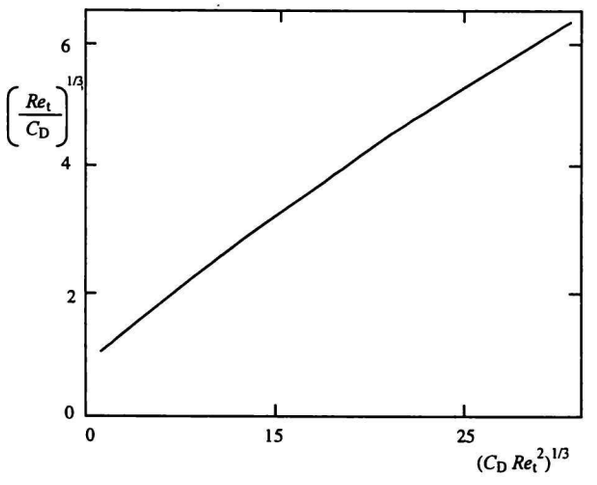

Fig. 5. Correlation plot for the terminal velocity. The line represents predictions of eqns (*10*) and (*11*).

when replotted in terms of Ar and Re_t. The whole set of the experimental results on the terminal velocity was correlated by the simple equation

$$Re_t = 0.1641 Ar^{0.7133} \qquad (6)$$

A very good fit of this relationship to the measured results is evident in Fig. 4. Of course, the empirical correlation (*6*) developed here has the usual limitations, and it should be applied with caution outside the experimental conditions from which it was educed.

An attempt has also been made to compare our results with the theoretical estimates for spherical particles [5, 14]

$$C_D Re_t^2 = (4/3) Ar \qquad (7)$$

where

$$C_D = (24/Re_t)(1 + 0.173 Re_t^{0.657}) + \\ + 0.413/(1 + 16\,300 Re_t^{-1.09}) \qquad (8)$$

A difference of approximately 20 % was observed between the predicted and the experimental values indicating that irregular sodium carbonate particles had a greater drag than the spherical ones.

In practice, a situation frequently occurs when the size of particles, which are just entrained under the operation conditions of interest, is to be determined. Successive approximations are needed for calculating the size of a particle which has a given terminal velocity when we employ the above relationship. To avoid the trial and error computations, the particle size must be eliminated from eqn (*7*).

Having introduced the dimensionless terminal velocity defined by the equation

$$Re_t^3/Ar = (4/3) Re_t/C_D = U_t^3 \rho_f^2/[g(\rho_s - \rho_f)\mu_f] \qquad (9)$$

one can note that the particle size does not occur on the right-hand side of eqn (*9*). On combining eqn (*6*) and (*9*) we get a relationship between the above dimensionless terminal velocity and the dimensionless diameter, $Ar = (3/4) C_D Re_t^2$, of a sodium carbonate particle

$$Re_t/C_D = 3.314 \times 10^{-3} Ar^{1.1399} \qquad (10)$$

or

$$Ar = 149.8 (Re_t/C_D)^{0.8773} \qquad (11)$$

The course of this function is shown in Fig. 5.

An operation region in which particles are fluidized, but not elutriated yet, can be expressed by the difference $Re_t - Re_{mf}$. Such quantities deduced from the experimental results in this study are plotted in Fig. 6. This contacting-mode diagram has practical implications in design of gas-solid contacting unit, where elutriation of particles is to be avoided or ensured. Any commercial fluidized bed unit processes particulate materials of real, more or less continuous size distribution. This fact can never be overlooked in either design or modelling efforts.

CONCLUSION

The minimum fluidization velocity and the terminal velocity of sodium carbonate decahydrate, sodium carbonate monohydrate, and anhydrous sodium carbonate were determined by experiment in dependence on the diameter of particles. Based on the collected experimental data, correlating equations were developed for the two fundamental characteristics of a fluidized bed. An explicit formula was also proposed that makes it possible to estimate the size of a carbonate particle which corresponds to a given terminal velocity under different conditions of operation. The presented find-

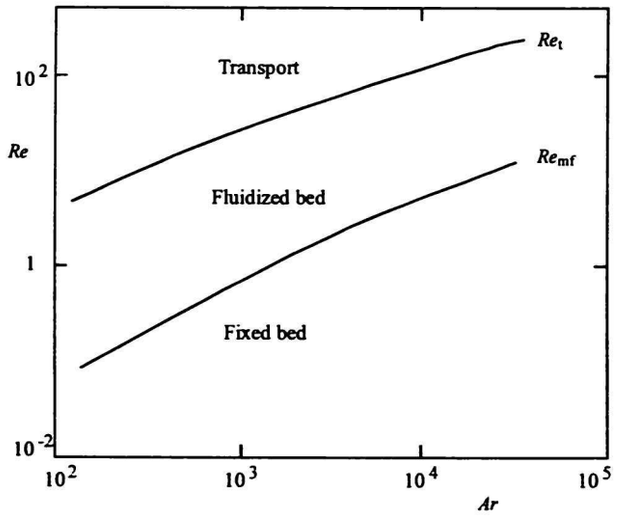

Fig. 6. Contacting-mode diagram for sodium carbonates particles. The lines represent predictions of eqns (*4*) and (*6*).

ings can readily be employed in successful design and operation of dense and circulating fluidized beds.

Acknowledgements. Financial support provided by the Grant Agency of the Czech Republic under the Grant No. 203/98/0101 and by the Grant Agency of the Academy of Sciences of the Czech Republic under the Grant No. A4072711 is gratefully acknowledged.

SYMBOLS

Ar	Archimedes number ($= d_p^3 g\rho_f(\rho_s - \rho_f)/\mu_f^2$)	
C_D	drag coefficient of a particle	
d_p	particle diameter	m
$\bar{d}_p$	mean particle over the very narrow size range	m
F	cross-sectional area of vessel	m^2
g	acceleration due to gravity ($= 9.807$ m s^{-2})	m s^{-2}
H	bed height	m
ΔH	increment of bed height	m
ΔP	pressure drop across the fluidized bed	Pa
Re_{mf}	Reynolds number at minimum fluidization velocity ($= U_{mf} d_p \rho_f / \mu_f$)	
Re_t	Reynolds number at terminal velocity of a particle ($= U_t d_p \rho_f / \mu_f$)	
U_{mf}	minimum fluidization velocity	m s^{-1}
U_t	terminal velocity	m s^{-1}
W	mass of particles	kg

Greek Letters

ε	bed voidage	
ε_{mf}	bed voidage at the point of minimum fluidization	
μ_f	fluid viscosity	Pa s, kg/(m s)
ρ_f	fluid density	kg m^{-3}
ρ_s	particle density	kg m^{-3}
ψ	particle sphericity, shape factor	

REFERENCES

1. Svoboda, K., Veselý, V., Hartman, M., and Jakubec, K., *Atmos. Protection 4*, 30 (1990).
2. Mocek, K., Stejskalová, K., Bach, P., Bastl, Z., Spirovová, I., and Erdös, E., *Collect. Czech. Chem. Commun. 61*, 825 (1996).
3. Hartman, M., Beran, Z., Svoboda, K., and Veselý, V., *Collect. Czech. Chem. Commun. 60*, 1 (1995).
4. Hartman, M. and Coughlin, R. W., *Collect. Czech. Chem. Commun. 58*, 1213 (1993).
5. Hartman, M. and Yates, J. G., *Collect. Czech. Chem. Commun. 58*, 961 (1993).
6. Pata, J. and Hartman, M., *Ind. Eng. Chem., Process Des. Dev. 17*, 231 (1978).
7. Pata, J. and Hartman, M., *Ind. Eng. Chem., Process Des. Dev. 19*, 98 (1980).
8. Hartman, M., Trnka, O., and Svoboda, K., *Ind. Eng. Chem. Res. 33*, 1979 (1994).
9. Svoboda, K. and Hartman, M., *Ind. Eng. Chem., Process Des. Dev. 20*, 319 (1981).
10. Ergun, S., *Chem. Eng. Prog. 48*, 89 (1952).
11. Yates, J. G., *Fundamentals of Fluidized-Bed Processes*. Butterworths, London, 1983.
12. Kunii, D. and Levenspiel, O., *Fluidization Engineering*. 2nd Edition. Butterworth—Heinemann, Boston, 1991.
13. Wen, C. Y. and Yu, Y. H., *Chem. Eng. Prog., Symp. Ser. 62*, 101 (1966).
14. Turton, R. and Levenspiel, O., *Powder Technol. 47*, 43 (1986).